APS physics

CHORUS

This is the accepted manuscript made available via CHORUS. The article has been published as:

High-pressure phases of boron arsenide with potential high thermal conductivity

Linyan Wang, Fei Tian, Xiaowei Liang, Yuhao Fu, Xufeng Mu, Jingying Sun, Xiang-Feng Zhou, Kun Luo, Yang Zhang, Zhisheng Zhao, Bo Xu, Zhifeng Ren, and Guoying Gao

Phys. Rev. B **99**, 174104 — Published 10 May 2019

DOI: 10.1103/PhysRevB.99.174104

High-pressure phases of boron arsenide with potential high thermal conductivity

Linyan Wang,[1] Fei Tian,[2] Xiaowei Liang,[1] Yuhao Fu,[3] Xufeng Mu,[1] Jingying Sun,[2] Xiang-Feng Zhou,[1] Kun Luo,[1] Yang Zhang,[1] Zhisheng Zhao,[1] Bo Xu,[1] Zhifeng Ren,[2,*] and Guoying Gao[1,†]

[1] *Center for High Pressure Science, State Key Laboratory of Metastable Materials Science and Technology, Yanshan University, Qinhuangdao 066004, China*

[2] *Department of Physics and the Texas Center for Superconductivity, University of Houston, Houston, TX 77204, USA*

[3] *State Key Laboratory of Superhard Materials, Key Laboratory of Automobile Materials of MOE, and College of Materials Science and Engineering, Jilin University, Changchun 130012, China*

(Dated: April 22, 2019)

Zinc-blende boron arsenide (BAs) has been confirmed to have impressively high thermal conductivity. However, studies on its phase transitions under pressure have been few. Here, through recently developed structure search method, we predicted that many polytypes with structural features of cubic- and hexagonal-diamond, which are known to be unstable even up to very high pressure for carbon and boron nitride, can become stable at low pressure and might be retained to ambient conditions. Moreover, some of these BAs polytypes are calculated to have impressively high thermal conductivities at ambient conditions and the thermal conductivities for zb- and 2H-BAs will decrease with the increasing pressure, which are mainly attributed to the stronger 3^{rd} anharmonic interaction. The current study will open up a new route to search for high thermal conductor.

Materials with high thermal conductivity (κ) are becoming increasingly important due to the huge demand for, and major challenge of, heat management in the modern micro- and nano-electronic industry[1]. Under the widely accepted criteria[2], the famous carbon allotropes of diamond and graphite have the highest κ ($\sim$2000 W m^{-1} K^{-1}) at room temperature (RT, $T = 300$ K) among bulk materials[3–5]. Unfortunately, synthesizing diamond is too expensive for practical applications, and graphite's anisotropy makes it unsuitable as well. Recently, zinc-blende boron arsenide (zb-BAs) was predicted to possess an exceptionally high κ over 2000 W m^{-1} K^{-1} at RT by first-principles calculations based on a band engineering method, which is comparable to that of diamond[6,7]. Subsequently, refined calculations[8] and experimental efforts on zb-BAs single crystal growth[9–11] have yielded a RT κ near 1300 W m^{-1} K^{-1}. These findings have attracted great interest in BAs and have provided a new view of high κ materials.

Represented by boron nitride (BN), high-pressure phase transitions of group III-V binary compounds have been systematically studied for decades. Due to the long-time lack of interest, though, there have been few studies on the phase transitions of BAs under high pressure. Experimentally, BAs was first synthesized in 1958 by direct reaction of B and As[12]. Since then, various approaches to synthesis of BAs starting from the elements have been reported[13–17]. At ambient environment (RT, 1 atm), BAs crystallizes in the zb structure with the space group of $F\bar{4}3m$[13]. Zinc-blende BAs is a semiconductor with an indirect electronic band gap of about 1.5-1.8 eV[18,19] and it is also a relatively hard material with Vickers hardness of 19 GPa[20]. As the temperature increases above 1193 K, zb-BAs becomes unstable and undergoes an irreversible decomposition to subarsenide, subsequently identified as $B_{12}As_2$[21]. Theoretically, the high-pressure phases of BAs have thus far been limited to structures such as NaCl, β-Sn, and CsCl phases[22]. The NaCl structure was calculated to be stable above 110 GPa. Experimentally, BAs has been reported to transform from the zb phase into an amorphous state at 125 GPa and room temperature, which does not undergo any further transition up to 165 GPa and persists as a metastable phase upon release of pressure[23]. No other structures have been either theoretically proposed or experimentally realized.

Here we report an extensive theoretical study on the phase transitions of BAs under pressure by the particle swarm optimization structural search method combined with first-principles calculations. Many new structures of BAs with the features of cubic- and hexagonal-diamond forms are found to be stable at pressure achievable in the laboratory. Interestingly, these new structures are calculated to potentially be ultrahigh κ materials, as well as hard materials, and also stable after releasing the pressure.

We performed an extensive search for the crystal structures of BAs under pressure by using the particle swarm optimization technique as implemented in the Crystal structure AnaLYsis by Particle Swarm Optimization (CALYPSO) code[24,25]. CALYPSO is a leading structure prediction method in the field and has successfully predicted the high-pressure structures of various systems[26–30]. The underlying *ab initio* structural relaxations were performed using density functional theory (DFT) within the Perdew-Burke-Ernzerhof (PBE) generalized gradient approximation (GGA)[31], as implemented in the Vienna *ab initio* simulation package (VASP) code[32]. The projector augmented wave (PAW) method was adopted, with $2s^2 2p^1$ and $4s^2 4p^3$ treated as valence electrons for B and As atoms, respectively. The kinetic cutoff energy of 1200 eV and corresponding Monkhorst-Pack (MP) k meshes for different structures were then adopted to ensure that the enthalpy converges to better than 0.01 meV/atom. The enthalpy values are

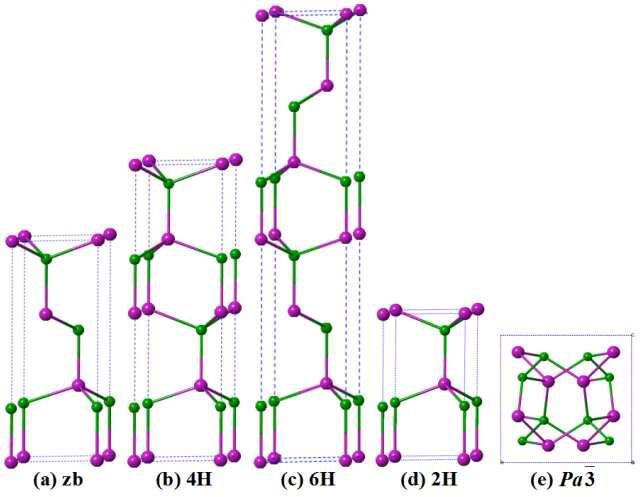

FIG. 1. The predicted high-pressure structures for BAs. The green and purple spheres represent the B and As atoms, respectively.

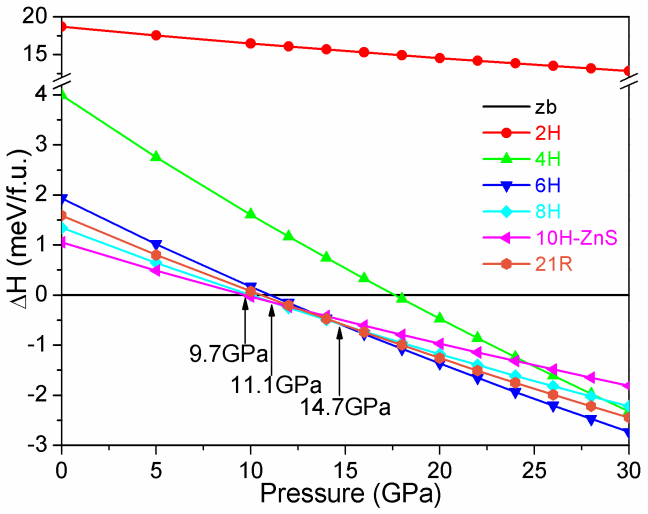

FIG. 2. The calculated enthalpies per formula unit of the hexagonal and rhombohedral diamond structures for BAs as a function of pressure with respect to the zb-BAs structure.

computed from H = U + PV (where H, U, P, and V are enthalpy, internal energy, pressure, and volume, respectively) by considering temperature as zero. Meta-GGA functional[33] was also adopted to check the accuracy of enthalpy differences of some structures calculated with PBE functional. The calculations for pressure versus volume curve of zb-BAs are performed using the full potential linearized augmented plane wave (FP-LAPW)[34] method as implemented in the WIEN2k code[35]. The band structures are calculated by hybrid functional calculations within Heyd-Scuseria-Ernzerhof (HSE) hybrid functional[36]. The phonon calculations were carried out by using a supercell approach within the PHONOPY code[37]. The Vickers hardness was estimated using the semiempirical hardness model for covalent crystals[38,39]. The lattice thermal conductivity κ was calculated by iteratively solving the phonon Boltzmann Transport equation as implemented in the ShengBTE package[40–42]. Further details on all computational methods are provided in the Supplemental Materials[43].

We began with the structure search at ambient pressure for BAs. At low pressure, the most stable structure is predicted to be the zb phase (Fig. 1a), which is in good agreement with the experimental observation. Moreover, the calculated lattice constant for zb-BAs of 4.817 Åis close to the measured value of 4.78 Å[14], which further supports the reliability of the current calculations. The zb structure contains perfect B and As tetrahedra with only B-As bonding. At 30 GPa, we predicted a hexagonal diamond structure with the space group of $P6_3mc$ (4H, Fig. 1b), which is also one of the polytypes for silicon carbide (SiC) at 1 atm. The 4H structure can be considered as the mixture of the cubic- and hexagonal- ($P6_3mc$, 2H) diamond characteristics, which is also similar to 4H hexagonal diamond. In addition, we also predicted several metastable 2H, 6H, 8H, and 9R hexagonal and rhombohedral diamond structures (Fig. 1c, d and S1a, b[43]). It is well known that many diamond polytypes containing large unit cells, such as 10H-ZnS, 15R, and 21R (Fig. S1c-e[43]), have been widely studied for SiC[44,45], C[46], and BN[47,48]. Therefore, these diamond polytypes containing large unit cells are very likely to become stable under pressure, and thus we also included them in the following enthalpy calculations. At 50 GPa, we predicted a simple-cubic structure, $Pa\bar{3}$ (Fig. 1e), with 8 f.u. in a unit cell, which is similar to BC8 Si. It should be noted that the B and As tetrahedra in the $Pa\bar{3}$ structure are distorted and that B-B bonds form in addition to the B-As bonds. At much higher pressure, all of the predicted structures show the separation of solid boron and arsenic layers (Fig. S2[43]), suggesting the trend of decomposition into the constituent solid elements.

The calculated enthalpy differences of the predicted structures relative to the zb-BAs are shown in Fig. 2. The 10H-ZnS structure is calculated to be stable with respect to the zb-BAs only above about 9.7 GPa, and the 8H and 6H structures then gradually become stable upon further compression. It should be noted that the enthalpy differences between these structures are only within a few meV, suggesting that all of these structures could be stable under high pressure. Interestingly, the metastable 2H structure might be also stable above 123 GPa with respect to the zb phase, as shown in Fig. S3[43]. This is extremely surprising given that previous theoretical calculations have indicated that 2H diamond and other diamond polytypes for carbon cannot be stable with respect to zb-diamond even up to very high pressure[46], which is also reproduced in the current work (Fig. S5a[43]). This is also the case for BN (Fig. S5b[43]). On the other hand, 2H diamond has been reported to be synthesized in 1967[49] even though production of a perfect crystal has not yet been reported, and many other diamond polytypes (6H,

8H, 10H-ZnS, 15R, and 21R) have also been found in experimental studies and in meteorites[50–56]. Therefore, it is probable that these diamond polytypes can be synthesized under pressure for BAs.

The 6H structure becomes stable at 14.7 GPa and remains stable until 54 GPa, above which it transforms into the 4H phase (Fig. S3[43]). At about 67 GPa, the 4H structure further transforms into the cubic $Pa\bar{3}$ phase, which is stable only within a very small pressure range of 67 to 74 GPa (Fig. S6a[43]), above which BAs will be stable in the structures with separated B and As layers. It should also be noted that BAs will become unstable relative to solid boron and arsenic above 27 GPa, (Fig. S6b[43]) but this does not preclude the possibility of observing the predicted diamond polytypes at lower pressure and at high temperature. From the calculated convex hull for the B-As system, which are in agreement with other theoretical results[57], even zb-BAs is also thermodynamically unstable relative to $B_{12}As_2$ and α-arsenic at ambient conditions (Figure S8[43]). However, zb-BAs is well known.

It is well known that zb-BAs is a semiconductor with an indirect band gap of 1.5-1.8 eV[18,19]. Thus, it is very interesting to study the electronic properties of these high-pressure phases. The predicted 2H, 4H, and 6H structures are all calculated to be semiconductors with indirect band gaps of about 1.1-1.2 eV (Fig. S9[43]), which are close to the calculated value of 1.19 eV for the zb phase. We know that the level of DFT usually underestimates band gaps. To get more reliable results, we also recalculated band gaps and band structures with the HSE hybrid functional, which employs a screened Coulomb potential for the exchange interaction. The recalculated band gap for the zb phase is 1.87 eV, which is in good agreement with previously theoretical and experimental results[18,19,58]. The recalculated band gaps for the 2H, 4H, and 6H structures improve to be of about 1.8-1.9 eV (Fig. 3). The similar semiconducting character of these high-pressure phases to that of the zb phase suggests that they might have additional similar properties, such as thermal conductivity.

To check the dynamical stability of these predicted structures, we studied their phonon spectra (Fig. 3 and Fig. S10[43]). No imaginary frequencies are found in these high-pressure phases at either high or ambient pressure, which suggests that they are also dynamically stable and might be retained to ambient condition if synthesized at high pressure and high temperature.

Recent theoretical and experimental studies confirm that zb-BAs has a high thermal conductivity over 1000 W m^{-1} K^{-1} at ambient conditions[9–11]. The ultrahigh κ observed in zb-BAs is mainly attributed to its combination of light B and heavy As atoms and satisfies the following rules: (i) the frequency gap between the acoustic phonons and optical phonons (a-o gap) is sufficiently large; and (ii) some of the acoustic phonons with different polarizations have regions of similar frequencies away from the Brillouin zone center. Therefore, we checked the

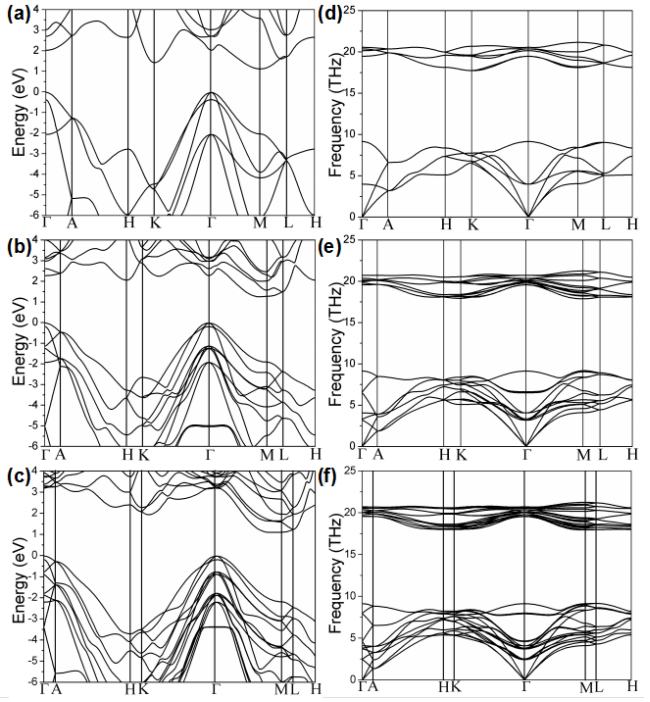

FIG. 3. The calculated electronic band structures of (a) 2H, (b) 4H, and (c) 6H at 1 atm for BAs using the HSE functional. The right panels (d), (e), and (f) show the calculated phonon spectra at 1 atm of the corresponding structure in the left panel.

phonon spectra of 2H-, 4H- and 6H-BAs carefully (Fig. 3). Unfortunately, there is no frequency gap between the acoustic and optical phonons. However, the three acoustic phonon modes in the 2H structure, which are mainly for heat-carrying, are away for the Brillouin zone center with the highest frequencies in the range of 3∼7 THz along Γ-A, Γ-K and Γ-M directions (Fig. 3d), which indicates a possible high thermal conductivity.

Fig. 4 shows the calculated κ as a function of temperature for diamond and BAs. Our calculated results for diamond are in excellent agreement with other theoretical results and available experimental data, which supports the validity of the current calculations. For zb-BAs, the calculated results are in good agreement with other theoretical results, though they are all higher than the experimental data[9–11]. Recent first-principles calculations incorporating four-phonon scattering predict a RT κ of 1400 W m^{-1} K^{-1}[8], and 1260 W m^{-1} K^{-1} when calculating a full solution of BTE[11], which agrees with the recent experimental data for zb-BAs[9–11]. Note that the calculated κ with three- or four-phonon scattering are both considered for the perfect BAs single crystal. In the experimentally synthesized single crystal zb-BAs samples, there are always defects and impurities, which will reduce the measured values of thermal conductivity. Particularly, the presence of As vacancy concentrations gives an anomalously strong suppression of the thermal conductivity[14,60]. Therefore, the predicted thermal con-

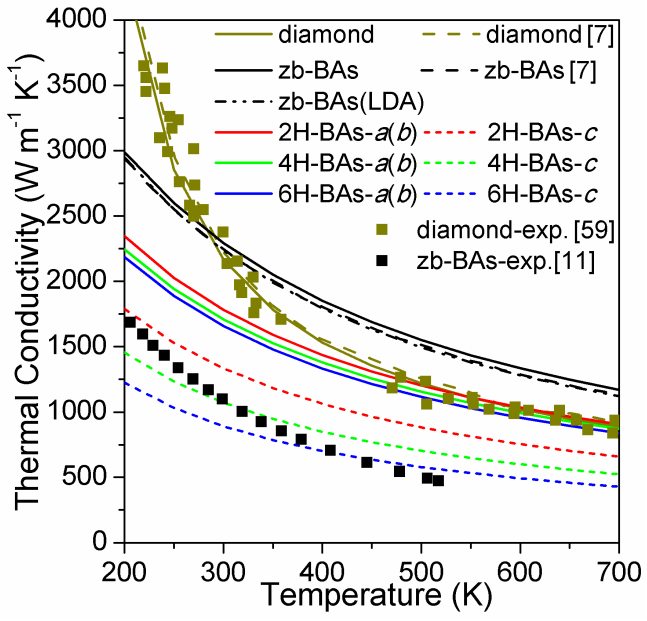

FIG. 4. Calculated temperature dependence of κ for diamond, and zb-, 2H-, 4H-, and 6H-BAs along the $a(b)$ (solid curves) and c (short-dashed curves) crystal axes. Calculated data from L. Lindsay *et al.*[7] are represented by the dashed curves. The κ of and zb-BAs using the local density approximation pseudopotential (dashed-dotted-dotted curves) were also calculated for comparison with the results from L. Lindsay *et al.*[7]. Measured κ values for diamond[59] and zb-BAs[11] are shown with scattered symbols.

ductivities for BAs with three-phonon scattering higher than the measured values are reasonable. Calculating thermal conductivity including four-phonon scattering is very complicated, time-consuming and the available results are still few. It will be the study topic in the future. Here, we only considered up to three-phonon scattering.

Surprisingly, the high-pressure 2H phase is predicted to exhibit κ of 1782 and 1335 W m^{-1} K^{-1} at RT along the $a(b)$ and c crystal axes, respectively, which suggests that the 2H phase is anisotropic. However, even the small κ of 1335 W m^{-1} K^{-1} is only lower than those of diamond and zb-BAs (Table 1). Since other diamond polytypes structures are close in enthalpy to the 2H structure, we also calculated the κ for 4H and 6H phases as examples. The calculated κ for 4H and 6H are 1710 and 1659 W m^{-1} K^{-1} along the $a(b)$ crystal axis, and 1072 and 891 W m^{-1} K^{-1} along the c crystal axis, respectively. It should be noted that the 4H and 6H phases are also anisotropic. The calculated κ along the $a(b)$ crystal axis for these hexagonal polytypes are all higher than the corresponding polytype along the c crystal axis over the temperature range considered. We find $\kappa_{2H} > \kappa_{4H} > \kappa_{6H}$ along both the $a(b)$ and c crystal axes. In these diamond polytypes, the larger number of atoms with increasing n in nH-BAs gives rise to an increasing number of low-lying optic branches, and the small phonon group velocities in these branches leads to lower κ with increasing n in nH-BAs (Fig. 3). Besides, from 2H to 4H to 6H, the calculated κ decreases slightly along the $a(b)$ axis and greatly along c, which is understandable when considering the more complex structure characteristics and complicated coupling between the acoustic and optical phonons for the structures with larger unit cells along the c crystal axis (see Table S1 for details[43]). However, the high-pressure phases of BAs at relatively low pressure are still good candidates for high thermal conductivity. This is the first time that possible high thermal conductivity has been predicted in a high-pressure phase for a material, which opens up a new route to search for high thermal conductors.

TABLE I. M_{av}, κ_{nat}, κ_{pure} (at 300 K), and percent enhancement to κ with isotopic purification given by $P = 100(\kappa_{pure}/\kappa_{nat}$ -1). The calculated κ of diamond, BN, zb-BAs and 2H-, 4H-, and 6H-BAs along the $a(b)$ and c crystal axes, respectively. The isotope concentrations (19.8% ^{10}B, 80.2% ^{11}B), (99.63% ^{14}N, 0.37% ^{15}N), and (98.9% ^{12}C, 1.1% ^{13}C) for these materials were considered to determine κ_{nat}. Measured values and calculated value of Refs.[7] for BN, BP, diamond, and zb-BAs with naturally occurring isotope concentrations are given in the *exp.* and *calc.* columns of κ_{nat}-ref, respectively.

	M_{av} (aum)	κ_{nat}-ref (W/m/K)		κ_{nat} (W/m/K)		κ_{pure} (W/m/K)		P	
		exp.	*calc.*						
Diamond	12.01	2270[a]	2290[b]	2166		3140		45	
BN	12.40	768[c]	940[b]	804		1963		144	
BP	20.89[b]	490[d]	580[b]			665[b]		15[b]	
zb-BAs	42.86	1300[e]	2240[b]	2293		3455		50	
				$a(b)$	c	$a(b)$	c	$a(b)$	c
2H-BAs	42.86			1782	1335	2580	1701	45	27
4H-BAs	42.86			1710	1072	2461	1341	44	25
6H-BAs	42.86			1659	891	2336	1089	41	22

[a] Refs.[4]
[b] Refs.[7]
[c] Refs.[61]
[d] Refs.[62,63]
[e] Refs.[9]

It is well known that the increase of pressure usually decreases the interatomic distances, which will increase the atomic vibrations and push phonon modes to higher frequencies. Thus, the thermal conductivity usually increases under pressure. Recently, the thermal conductivities as a function of pressure for many materials have been studied[64–69]. For example, under pressure, κ for diamond, BN, MgO and AlN increase, while κ for HgTe, BeTe and BSb decrease and CdTe and ZnTe remain constant. In addition, κ for ZnO, GaN and BeSe even exhibit nonmonotonic dependence on pressure. Therefore, the pressure dependence of the thermal conductivity is very complicated and the study of the thermal conductivity for BAs under pressure is necessary. Fig. 5 shows the calculated κ_{nat} and κ_{pure} as a function of pressure for zb- and 2H-BAs at 300 K. The calculated κ_{nat} and κ_{pure} for zb-BAs decreases with pressure, which is in

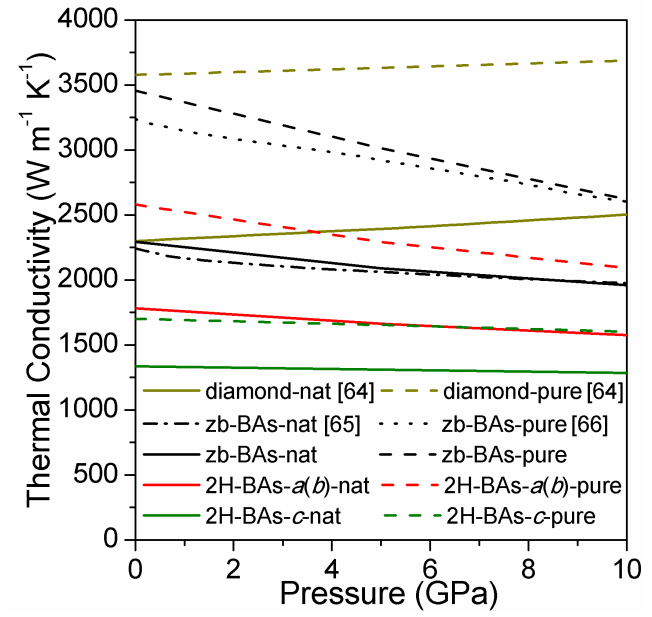

FIG. 5. Calculated pressure dependence of κ for zb- (black curves) and 2H-BAs along the $a(b)$ (red curves) and c (green curves) crystal axes at 300 K. κ_{nat} are represented by solid curves, while κ_{pure} are represented by dashed curves. Calculated κ_{nat} and κ_{pure} for diamond[64] are represented by the solid and dashed dark yellow curves, respectively. Calculated κ_{nat}[65] and κ_{pure}[66] for zb-BAs are represented by dashed-doted and dotted black curves, respectively.

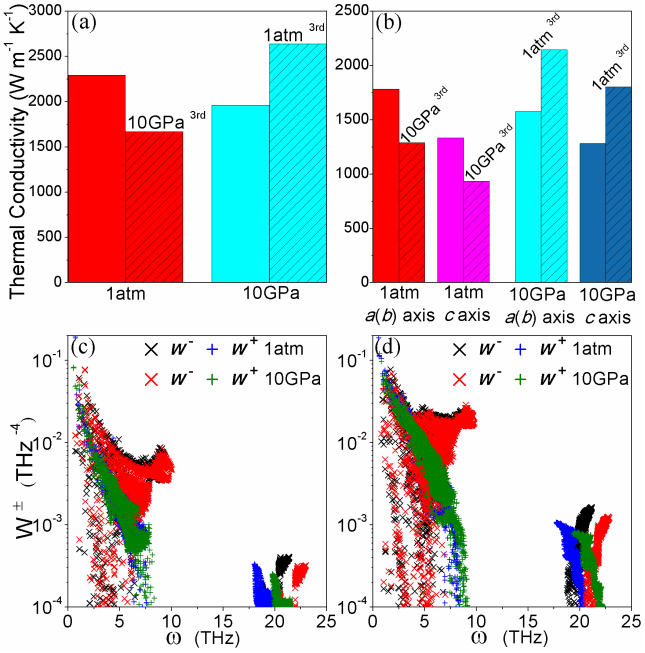

FIG. 6. Calculated κ by interchanging the anharmonic IFCs at 1 atm and 10 GPa for (a) zb- and (b) 2H-BAs at 300 K. Calculated three-phonon scattering phase space at 1 atm (soild circles) and 10 GPa (open uptriangles) for (c) zb- and (d) 2H-BAs at 300 K.

good agreement with the previous theoretical calculation with three-phonon scattering[65,66]. The calculated thermal conductivity for 2H-BAs also decreases under pressure but decreases a little. In general, the thermal conductivities with the same structures are known to be dominated by the 3^{rd} anharmonic interaction and the three-phonon scattering phase space $W^{\pm}$. To investigate the influences of third-order anharmonic interatomic force constants (IFCs) on changing three-phonon anharmonic scattering processes, we calculated κ by deliberately interchanging the anharmonic IFCs between the cases at 1 atm and 10 GPa, as shown in Fig. 6a and 6b. For zb- and 2H-BAs at 1 atm, when replacing the anharmonic IFCs with the ones from 10 GPa and keeping the other quantities unchanged, we find that κ decreases, whereas κ for 10 GPa increases when using the anharmonic IFCs from 1 atm. As we know, the anharmonic scattering rates are generally proportional to the square of the anharmonic IFCs. Thus, the anharmonic IFCs of zb- and 2H-BAs at 10 GPa are both larger than the corresponding values at 1 atm, leading to the higher anharmonic scattering rates and thus lower κ at 10 GPa. On the other hand, three-phonon scattering phase space $W^{\pm}$ represent the contribution of harmonic phonon frequencies to the anharmonic scattering rates, and it consists of two components corresponding to absorption (W^+, two phonons merging into one) and emission (W^-, one phonon splitting into two) processes. As shown in Fig. 6c and 6d, W^+ and W^- of zb- and 2H-BAs at 10 GPa are nearly same as the corresponding values at 1 atm in the low-frequency (<10 THz) region, while a little smaller than the corresponding values at 1 atm in the high-frequency region about 20 THz. Thus, the small decrease in $W^{\pm}$ with increasing pressure leads to the small increase in thermal conductivity. However, the decrease of κ resulted from the stronger 3^{rd} anharmonic interaction prevail against the increase of κ owing to slightly decreasing $W^{\pm}$, giving decreasing κ under pressure. As we mentioned above, the thermal conductivity of many materials, such as diamond, would increase under pressure. The primary mechanism for the enhancement of κ under pressure for diamond is the decrease in the 3^{rd} anharmonic interaction between phonons[64]. However, the 3^{rd} anharmonic interaction increases with pressure for zb- and 2H-BAs, which will lead to the decrease in κ. In addition, the influence of the three-phonon scattering phase space between acoustic phonons[65], acoustic and optic phonons as well as optic phonons on thermal conductivity are also studied. However, the increase in 3^{rd} anharmonic interaction under pressure is the dominated parameter for the negative pressure dependent thermal conductivity for zb- and 2H-BAs.

Zb-BAs is also a relatively hard material with a measured Vickers hardness of 19 GPa[20]. Our calculated Vickers hardness for zb-BAs is 20 GPa, which is in good agreement with experimental results[20] and previous theoretical calculations[70]. The calculated Vickers hardness

TABLE II. The calculated Vickers hardness of 2H, 4H, 6H, and $Pa\bar{3}$ phases for BAs.

	2H	4H	6H	$Pa\bar{3}$
H_v(GPa)	21.2	21.6	21.6	20.1

values of high-pressure phases (2H, 4H, 6H, and $Pa\bar{3}$) are listed in Table 2. It can be seen that all of the high-pressure phases are calculated to exhibit a Vickers hardness of about 21 GPa, which is also close to that of the zb phase at ambient conditions. Therefore, the high-pressure phases of BAs are also potentially hard materials.

In summary, we conducted an extensive study of the high-pressure phases for BAs and predicted many stable diamond polytypes at pressures easily achievable in the laboratory. It is interesting to note that these diamond polytypes for BAs have the same structural characteristics with cubic- and hexagonal-diamond and are calculated to be good candidates for high thermal conductivity, as well as high hardness. The pressure dependence of the thermal conductivity for zb- and 2H-BAs is also investigated and the underlying origins are discussed. The current study will open a new route for the exploration of high thermal conductivity materials in high-pressure phases.

ACKNOWLEDGMENTS

F. Tian and Z. Ren thank David Broido for his valuable discussions. The work was supported by the National Natural Science Foundation of China (Grant 11604290 and 51732010), the Office of Naval Research under MURI grant N00014-16-1-2436, the Science Foundation for the Youth Top-notch Talent from Universities of Hebei Province (Grant BJ2017023), the Funding Program for Recruited Oversea Scholars of Hebei Province (CL201729), and the PhD foundation by Yanshan University (Grant B970).

L. Wang and F. Tian contributed equally to this work.

* zren@uh.edu
† gaoguoying@ysu.edu.cn

[1] M. M. Waldrop, Nature **530**, 144 (2016).
[2] G. A. Slack, J. Phys. Chem. Solids **34**, 321 (1973).
[3] J. R. Olson, R. O. Pohl, J. W. Vandersande, A. Zoltan, T. R. Anthony, and W. F. Banholzer, Phys. Rev. B **47**, 14850 (1993).
[4] L. Wei, P. K. Kuo, R. L. Thomas, T. R. Anthony, and W. F. Banholzer, Phys. Rev. Lett. **70**, 3764 (1993).
[5] T. L. Bergman, F. P. Incropera, D. P. DeWitt, and A. S. Lavine, *Fundamentals of heat and mass transfer* (John Wiley Sons, 2011).
[6] D. A. Broido, L. Lindsay, and T. L. Reinecke, Phys. Rev. B **88**, 214303 (2013).
[7] L. Lindsay, D. A. Broido, and T. L. Reinecke, Phys. Rev. Lett. **111**, 025901 (2013).
[8] T. Feng, L. Lindsay, and X. Ruan, Phys. Rev. B **96**, 161201 (2017).
[9] J. S. Kang, M. Li, H. Wu, H. Nguyen, and Y. Hu, Science **361**, 575 (2018).
[10] S. Li, Q. Zheng, Y. Lv, X. Liu, X. Wang, P. Y. Huang, D. G. Cahill, and B. Lv, Science **361**, 579 (2018).
[11] F. Tian, B. Song, X. Chen, N. K. Ravichandran, Y. Lv, K. Chen, S. Sullivan, J. Kim, Y. Zhou, T.-H. Liu, M. Goni, Z. Ding, J. Sun, G. A. G. Udalamatta Gamage, H. Sun, H. Ziyaee, S. Huyan, L. Deng, J. Zhou, A. J. Schmidt, S. Chen, C.-W. Chu, P. Y. Huang, D. Broido, L. Shi, G. Chen, and Z. Ren, Science **361**, 582 (2018).
[12] J. A. Perri, S. La Placa, and B. Post, Acta Crystallogr. **11**, 310 (1958).
[13] T. L. Chu and A. E. Hyslop, J. Appl. Phys. **43**, 276 (1972).
[14] B. Lv, Y. Lan, X. Wang, Q. Zhang, Y. Hu, A. J. Jacobson, D. Broido, G. Chen, Z. Ren, and C.-W. Chu, Appl. Phys. Lett. **106**, 074105 (2015).
[15] F. Tian, B. Song, B. Lv, J. Sun, S. Huyan, Q. Wu, J. Mao, Y. Ni, Z. Ding, S. Huberman, T.-H. Liu, G. Chen, S. Chen, C.-W. Chu, and Z. Ren, Appl. Phys. Lett. **112**, 031903 (2018).
[16] J. Xing, X. Chen, Y. Zhou, J. C. Culbertson, J. A. Freitas, E. R. Glaser, J. Zhou, L. Shi, and N. Ni, Appl. Phys. Lett. **112**, 261901 (2018).
[17] J. Xing, E. R. Glaser, B. Song, J. C. Culbertson, J. A. Freitas, R. A. Duncan, K. A. Nelson, G. Chen, and N. Ni, Appl. Phys. Lett. **112**, 241903 (2018).
[18] S. Wang, S. F. Swingle, H. Ye, F.-R. F. Fan, A. H. Cowley, and A. J. Bard, J. Am. Chem. Soc. **134**, 11056 (2012).
[19] J. L. Lyons, J. B. Varley, E. R. Glaser, J. A. Freitas, J. C. Culbertson, F. Tian, G. A. Gamage, H. Sun, H. Ziyaee, and Z. Ren, Appl. Phys. Lett. **113**, 251902 (2018).
[20] R. C. Weast, *Handbook of Chemical Physics, 69th Edition.* (CRC Press, 1989).
[21] F. V. Williams and R. A. Ruehrwein, J. Am. Chem. Soc. **82**, 1330 (1960).
[22] R. M. Wentzcovitch, M. L. Cohen, and P. K. Lam, Phys. Rev. B **36**, 6058 (1987).
[23] R. G. Greene, H. Luo, A. L. Ruoff, S. S. Trail, and F. J. DiSalvo, Phys. Rev. Lett. **73**, 2476 (1994).
[24] Y. Wang, J. Lv, L. Zhu, and Y. Ma, Phys. Rev. B **82**, 094116 (2010).
[25] Y. Wang, J. Lv, L. Zhu, and Y. Ma, Comput. Phys. Commun. **183**, 2063 (2012).
[26] Y. Li, J. Hao, H. Liu, Y. Li, and Y. Ma, J. Chem. Phys. **140**, 174712 (2014).
[27] L. Zhu, H. Liu, C. J. Pickard, G. Zou, and Y. Ma, Nat. Chem. **6**, 644 (2014).
[28] J. Lv, Y. Wang, L. Zhu, and Y. Ma, Phys. Rev. Lett. **106**, 015503 (2011).
[29] J. Lin, S. Zhang, W. Guan, G. Yang, and Y. Ma, J. Am. Chem. Soc. **140**, 9545 (2018).
[30] Z. Zhao, S. Zhang, T. Yu, H. Xu, A. Bergara, and G. Yang,

Phys. Rev. Lett. **122**, 097002 (2019).
[31] J. P. Perdew, K. Burke, and M. Ernzerhof, Phys. Rev. Lett. **77**, 3865 (1996).
[32] G. Kresse and J. Furthmüller, Phys. Rev. B **54**, 11169 (1996).
[33] J. Sun, M. Marsman, G. I. Csonka, A. Ruzsinszky, P. Hao, Y.-S. Kim, G. Kresse, and J. P. Perdew, Phys. Rev. B **84**, 035117 (2011).
[34] J. C. Slater, *Statistical Exchange-Correlation in the Self-Consistent Field* (Academic Press, 1972).
[35] K. Schwarz and P. Blaha, Comput. Mater. Sci. **28**, 259 (2003).
[36] J. Heyd, G. E. Scuseria, and M. Ernzerhof, J. Chem. Phys. **118**, 8207 (2003).
[37] S. Baroni, P. Giannozzi, and A. Testa, Phys. Rev. Lett. **58**, 1861 (1987).
[38] F. Gao, J. He, E. Wu, S. Liu, D. Yu, D. Li, S. Zhang, and Y. Tian, Phys. Rev. Lett. **91**, 015502 (2003).
[39] J. He, E. Wu, H. Wang, R. Liu, and Y. Tian, Phys. Rev. Lett. **94**, 015504 (2005).
[40] W. Li, L. Lindsay, D. A. Broido, D. A. Stewart, and N. Mingo, Phys. Rev. B **86**, 174307 (2012).
[41] W. Li, J. Carrete, N. A. Katcho, and N. Mingo, Comput. Phys. Commun. **185**, 1747 (2014).
[42] W. Li and N. Mingo, Phys. Rev. B **89**, 184304 (2014).
[43] See Supplemental Material at *** for further computational details, the diamond polytypes structures and predicted structures at high pressure of BAs, the calculated enthalpies curves for BAs, C, and BN, convex hull for the B-As system, electronic band structure and phonon spectra for BAs and structural information, which includes Refs.[24,25,31–35,37–42,57,71–74].
[44] P. Käckell, B. Wenzien, and F. Bechstedt, Phys. Rev. B **50**, 17037 (1994).
[45] A. Mujica, A. Rubio, A. Muñoz, and R. J. Needs, Rev. Mod. Phys. **75**, 863 (2003).
[46] B. Wen, J. Zhao, M. J. Bucknum, P. Yao, and T. Li, Diam. Relat. Mater. **17**, 356 (2008).
[47] S. Komatsu, K. Okada, Y. Shimizu, and Y. Moriyoshi, J. Phys. Chem. B **103**, 3289 (1999).
[48] S. Komatsu, K. Kobayashi, Y. Sato, D. Hirano, T. Nakamura, T. Nagata, T. Chikyo, T. Watanabe, T. Takizawa, K. Nakamura, and T. Hashimoto, J. Phys. Chem. C **114**, 13176 (2010).
[49] F. P. Bundy and J. S. Kasper, J. Chem. Phys. **46**, 3437 (1967).
[50] M. Frenklach, R. Kematick, D. Huang, W. Howard, K. E. Spear, A. W. Phelps, and R. Koba, J. Appl. Phys. **66**, 395 (1989).
[51] S. Bhargava, H. D. Bist, S. Sahli, M. Aslam, and H. B. Tripathi, Appl. Phys. Lett. **67**, 1706 (1995).
[52] R. Kapil, B. R. Mehta, and V. D. Vankar, Appl. Phys. Lett. **68**, 2520 (1996).
[53] A. K. Sharma, H. G. Salunke, G. P. Das, P. Ayyub, and M. S. Multani, J. Phys. Condens. Matter **8**, 5801 (1996).
[54] Y. G. Gogotsi, A. Kailer, and K. G. Nickel, J. Appl. Phys. **84**, 1299 (1998).
[55] R. Kapil, B. Mehta, and V. Vankar, Thin Solid Films **312**, 106 (1998).
[56] Y. Lifshitz, X. F. Duan, N. G. Shang, Q. Li, L. Wan, I. Bello, and S. Lee, Nature **412**, 404 (2001).
[57] A. Ektarawong, S. I. Simak, and B. Alling, Phys. Rev. B **96**, 024202 (2017).
[58] S. Chae, K. Mengle, J. T. Heron, and E. Kioupakis, Appl. Phys. Lett. **113**, 212101 (2018).
[59] D. G. Onn, A. Witek, Y. Z. Qiu, T. R. Anthony, and W. F. Banholzer, Phys. Rev. Lett. **68**, 2806 (1992).
[60] N. H. Protik, J. Carrete, N. A. Katcho, N. Mingo, and D. Broido, Phys. Rev. B **94**, 045207 (2016).
[61] N. V. Novikov, T. D. Osetinskaya, A. A. Shul zhenko, A. P. Podoba, A. N. Sokolov, and I. A. Petrusha, Dopov. Akad. Nauk Ukr. RSR, Ser. A: Fiz.-Tekh. Mat. Nauki **72** (1983).
[62] J. S. Kang, H. Wu, and Y. Hu, Nano Lett. **17**, 7507 (2017).
[63] Q. Zheng, S. Li, C. Li, Y. Lv, X. Liu, P. Y. Huang, D. A. Broido, B. Lv, and D. G. Cahill, Adv. Funct. Mater. **28**, 1805116 (2018).
[64] D. A. Broido, L. Lindsay, and A. Ward, Phys. Rev. B **86**, 115203 (2012).
[65] N. K. Ravichandran and D. Broido, Nat. Commun. **10**, 827 (2019).
[66] L. Lindsay, D. A. Broido, J. Carrete, N. Mingo, and T. L. Reinecke, Phys. Rev. B **91**, 121202 (2015).
[67] S. Mukhopadhyay and D. A. Stewart, Phys. Rev. Lett. **113**, 025901 (2014).
[68] T. Ouyang and M. Hu, Phys. Rev. B **92**, 235204 (2015).
[69] K. Yuan, X. Zhang, D. Tang, and M. Hu, Phys. Rev. B **98**, 144303 (2018).
[70] F. Gao, Phys. Rev. B **73**, 132104 (2006).
[71] D. M. Ceperley and B. J. Alder, Phys. Rev. Lett. **45**, 566 (1980).
[72] M. D. Segall, P. J. D. Lindan, M. J. Probert, C. J. Pickard, P. J. Hasnip, S. J. Clark, and M. C. Payne, J. Phys. Condens. Matter **14**, 2717 (2002).
[73] D. Sánchez-Portal, E. Artacho, and J. M. Soler, Solid State Commun. **95**, 685 (1995).
[74] D. Sánchez-Portal, E. Artacho, and J. M. Soler, J. Phys. Condens. Matter **8**, 3859 (1996).